IEEE Control Systems Letters paper presented at
2023 62nd IEEE Conference on Decision and Control (CDC)
December 13-15, 2023. Marina Bay Sands, Singapore

Rapid transfer alignment for large and time-varying attitude misaligment angles

Laetitia Tosoni, Minh Tu Pham, Paolo Massioni and Elliot Broussard

Abstract— **Transfer alignment is an effective method to estimate the attitude difference between two inertial platforms. Traditional transfer alignment methods are either meant for small misalignments or use nonlinear filtering. Linear methods for large misalignments use quaternion attitude representation, but their performance degrades when the misalignment is not constant or slowly varying. This work proposes applying rapid transfer alignment to the inertial stabilization of a Satcom On-The-Move antenna. In this application case, the two inertial platforms are connected by a kinematic chain, meaning the attitude difference between the inertial platforms is both large and time-varying. This work proposes a method to estimate this attitude difference, with a Kalman filter used for the estimation of the unknown angles. To that effect, a new propagation model is developed to take into account the misalignment variations using master and slave rotation rates. Simulation results show the performance of the proposed solution in a Satcom antenna inertial stabilization case.**

I. Introduction

Inertial navigation algorithms provide an effective means to compute the attitude and position of vehicles (aircraft, ships, etc.) [1]. In some applications, a subpart of the vehicle can be equipped with its own navigation system: the most common example is weapons carried by an aircraft.

In a projectile application [1], the final objective is for the projectile to follow its intended trajectory. The aircraft's aiming systems rely on the main inertial navigation system (INS) information to calculate said trajectory. As a consequence, the projectile's own inertial measurement unit (IMU) must be aligned with the main INS to follow that trajectory after launch. Transfer alignment algorithms have been originally developed to ensure that the projectile's navigation system worked in the same reference frame as the aiming system. To do so, transfer alignment algorithms estimate the misalignment between a high-grade INS, located on the carrier vehicle, and a low-cost IMU, located on the missile.

In addition to the original projectile applications, other applications exist, such as aircraft carried by a ship as in [2], remote sensors carried by an aircraft as in [3], or spacecraft launched from a mobile base as studied in [4].

The principle of transfer alignment is as follows. Two inertial measurement units, a master INS and a slave IMU, exist in different reference frames as part of a single vehicle. They both measure the same variable, each in their own reference frame. These two measurements are compared in order to deduce the orientation difference between their reference frames.

Several methods of transfer alignment exist, and they are usually classified based on the type of measurement the estimator uses as inputs. According to [1], rotation rate, attitude, velocity or acceleration are the most common methods. Combinations of several measurements are also used: the technique known as rapid transfer alignment, first described by [5], uses a combination of attitude and velocity measurements. It allows a very fast and very precise estimation (estimation error of less than 1 mrad within 10 seconds), and according to [6], it is regarded as the best transfer alignment technique. However, it estimates a small, constant misalignment angle, and it uses small angle approximation to linearize the model. As a consequence, the larger the misalignment, the more the algorithm's performances degrade. Furthermore, potential variations in the misalignment angle are not taken into account by the model.

Following the advent of rapid transfer alignment, efforts were made to reduce the computational load of the algorithm, as done in [7], and to compensate the carrier flexure, as done in [8]. Carrier flexure is the rapid change of misalignment angle due to vibrations and deformations between the master INS and the slave IMU, and it impacts the accuracy of the estimation when not taken in consideration. These methods are still applied to a small and constant misalignment angle, and suffer from the drawbacks previously mentioned.

Several methods exist to estimate large misalignment angles. Some use non-linear filtering, such as the unscented Kalman filter [9] or the extended Kalman filter [10]. However, works such as [11] and [12] managed to estimate a large misalignment angle with a linear Kalman filter, by using a quaternion attitude representation instead of Euler angles. In all these cases, however, the estimated misalignment remained constant, and the model was not built to take into account potential variations.

In this work, transfer alignment is applied to the inertial stabilization of a satellite communication antenna (called Satcom On-The-Move, or SOTM). As presented in [13], in order to obtain high data rates, the antenna must be directional, which means that the received and emitted electromagnetic waves are oriented in a specific direction of space, called the line of sight or boresight. The line of sight must be steered in order to be aligned with the satellite to ensure a sufficient data rate transfer. The accuracy with which the antenna must be pointed depends on the antenna size and the radiofrequency band used to communicate.

In order to keep the antenna pointed towards the satellite, it is mounted on an Antenna Positioning System (APS). The APS is made of several axes actuated by servomotors. In our application case, the APS has two axes: an azimuth axis, and an elevation axis. In order to control the APS, the line of

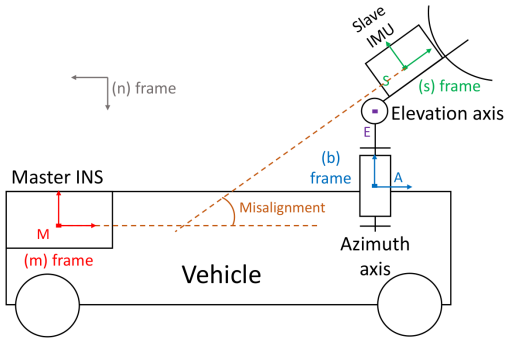

Fig. 1. Structure of the antenna positioning system

sight's current direction must be known; as a consequence, a slave IMU is aligned with the antenna's line-of sight. Placing the IMU in the same reference frame as the line of sight minimizes the risks of assembly misalignment errors. The master INS is located on the vehicle. As seen in Fig. 1, the APS can create a large and time-varying orientation difference between the master and the slave inertial sensors. In the currently existing transfer alignment algorithms, this variation is an important perturbation that is not accounted for by the models.

The contribution of the proposed method relies on the inclusion of the propagation model for the movements of the secondary IMU, namely the one that is connected to the antenna in our application. This makes the method directly applicable to all cases where large relative, time-varying angles are featured between the two platforms; this case is usually neglected in other transfer alignment methods, due to the fact that the two platforms are connected to the same rigid body. Specifically, this does not mean that the former algorithms cannot be used for tracking antenna movements; it means though that they will need to be tuned in a way that the propagation dynamics is considered as an unknown disturbance, which is inefficient. Adding the propagation model makes it unnecessary to do this step, making an efficient and performing tuning of the filter quite easy and direct.

This article is organized as follows. Section II specifies the quaternion properties and different reference frames that will be used in the model. Section III presents the measurement model, the propagation model and the lever arm compensation of the transfer alignment algorithm. The lever arm compensation is meant to take into consideration the physical distance between the master and slave systems, and its impact on velocity measurements. Section IV presents the simulation conditions and the results that confirm the effectiveness of the proposed method for our purposes, and then some comclusions are presented in Section V.

II. Preliminaries

A. Nomenclature

- q_k^j: quaternion expressing the rotation from frame k to frame j
- C_k^j: rotation matrix from frame k to frame j
- $\bar{q}$ the quaternion conjugate of q
- For a quaternion q, we write q_0 for its scalar part and $\vec{q}$ for its vector part such as $q = \begin{bmatrix} q_0 & \vec{q}^T \end{bmatrix}^T$. The vector part is made of three terms such as $\vec{q} = \begin{bmatrix} q_1 & q_2 & q_3 \end{bmatrix}^T$
- $C(q)$: rotation matrix representing the same orientation as the attitude quaternion q
- $\vec{\omega}_{j/k}^l$: rotation rate of frame j relative to frame k expressed in coordinate frame l
- $\vec{a}_{j/k}^l$: acceleration of frame j relative to frame k expressed in coordinate frame l
- $\vec{v}_{j/k}^l$: velocity of frame j relative to frame k expressed in coordinate frame l
- $\vec{g}^n$: gravity acceleration in coordinate frame n
- $\vec{f}^s$: acceleration sensed by the slave IMU such as $\vec{f}^s = \vec{a}_{s/n}^s + \vec{g}^s$
- θ_{Az}: rotation angle about the azimuth axis
- θ_{El}: rotation angle about the elevation axis
- $S(\vec{u})$: 3-by-3 skew-symmetric matrix associated with a 3-by-1 vector $\vec{u}$: $S(\vec{u}) = \begin{bmatrix} 0 & -u_3 & u_2 \\ u_3 & 0 & -u_1 \\ -u_2 & u_1 & 0 \end{bmatrix}$
- $\dot{x}$: derivative of variable x with respect to time
- $\hat{x}$: estimation of variable x

B. Quaternion attitude representation

Unit-norm quaternions can be used to represent attitude [14]. They are more compact than rotation matrices, and unlike Euler angles, they avoid gimbal lock issues.

Five properties are key for attitude quaternions. The first one is their derivative [14]:

$$\dot{q}_k^j = \frac{1}{2} q_k^j \otimes \omega_{k/j}^k \tag{1}$$

where $\otimes$ is the Hamilton product between two quaternions, q_k^j is the attitude quaternion from frame k to frame j, $\vec{\omega}_{j/k}^l$ is the rotation rate of j relative to k expressed in l, and for any rotation rate $\vec{\omega}_{k/j}^k$, $\omega_{k/j}^k$ is the associated quaternion such as $\omega_{k/j}^k = \begin{bmatrix} 0 & \vec{\omega}_{k/j}^{k\,T} \end{bmatrix}^T$.

The second one is the use of attitude quaternion to change another quaternion's coordinate frame. For example, with rotation rates:

$$\omega_{j/k}^o = q_l^o \otimes \omega_{j/k}^l \otimes q_o^l. \tag{2}$$

The third one is the conjugate of an attitude quaternion, with $\bar{q}$ the conjugate of q:

$$\bar{q}_k^j = q_j^k. \tag{3}$$

Therefore,

$$q_k^j \otimes q_j^k = \begin{bmatrix} 1 & 0 & 0 & 0 \end{bmatrix}^T \tag{4}$$

with $\begin{bmatrix} 1 & 0 & 0 & 0 \end{bmatrix}^T$ being the multiplicative identity for the quaternion algebra.

The fourth one is the matrix form expression of quaternion multiplication. For any two quaternions q and p:

$$\gamma(q) = \begin{pmatrix} q_0 & -\vec{q}^T \\ \vec{q} & q_0 I + S(\vec{q}) \end{pmatrix} \quad (5)$$

$$\chi(p) = \begin{pmatrix} p_0 & -\vec{p}^T \\ \vec{p} & p_0 I - S(\vec{p}) \end{pmatrix} \quad (6)$$

$$q \otimes p = \gamma(q)p = \chi(p)q. \quad (7)$$

with I the 3-by-3 identity matrix.

The last property is the conversion from attitude quaternion to other attitude representations. A quaternion can be converted to a rotation matrix or to Euler angles for better readability. In this paper, we will display results in Euler angles using the ZYX convention.

C. Reference frames

The reference frames used in this paper are the same as in [12]. They are illustrated in Fig. 1 and defined as follows.

- NED frame (n): Local North-East-Down frame.
- NED frame at start time (n_0): Local North-East-Down frame at the start of transfer alignment. This frame is non-rotating with regard to inertial frame.
- Master INS body frame (m): Orthogonal reference frame aligned with master INS axes.
- Bearing body frame (b): Reference frame originating at the base of the azimuth joint, stemming from the rotation of (m) around the azimuth axis.
- Slave IMU body frame (s): Orthogonal reference frame aligned with slave IMU axes.
- Slave IMU body frame at the start time (s_0): It coincides with the slave INS body frame at the start of transfer alignment. It does not rotate relative to an inertial frame.
- Earth frame (e): Geocentric frame.
- Inertial frame (i): Frame considered non-rotating and unmoving for the entirety of the transfer alignment.

III. Rapid transfer alignment algorithm for SOTM

In traditional transfer alignment, the master INS and slave IMU measure the same variable in their respective reference frame. In this work's application case, the two inertial platforms are separated by a kinematic chain. This kinematic chain's motion will induce a specific velocity difference between the slave and the master, and will therefore need to be compensated. It can also cause large and time-varying attitude differences between the master frame and slave frame.

In this section, the algorithm's structure is described, then the measurement and propagation equations are given. Lever arm compensation and integration method for the measurement equation are taken into consideration.

A. Algorithm structure

A linear system can be defined with a measurement matrix H and a propagation matrix A. Using these matrices and a measurement vector Y, it is possible to estimate the system's state vector X with the linear equations:

$$\begin{cases} \dot{X} = AX \\ Y = HX. \end{cases} \quad (8)$$

The state vector to be estimated is:

$$X = \begin{bmatrix} q_{s_0}^{n_0} \\ q_s^m \end{bmatrix} \quad (9)$$

with $q_{s_0}^{n_0}$ being the attitude of frame (s) relative to frame (n) at $t = 0$, and q_s^m being the attitude of (s) relative to (m) at the current time.

The inputs of the algorithm are as follows:

- $\vec{v}_{m/e}^{\,n}$: the master velocity provided by the master INS
- $\vec{\omega}_{m/n}^{\,m}$: the master rotation rate provided by the master INS
- q_m^n: the master attitude provided by the master INS
- $\vec{f}^{\,s}$: the slave accelerometers output provided by the slave IMU
- $\vec{\omega}_{s/s0}^{\,s}$: the slave rotation rate provided by the slave IMU
- θ_{Az} and θ_{El}: azimuth and elevation angles provided by the APS encoders, which can yield $\dot{\theta}_{Az}$ and $\dot{\theta}_{El}$ through derivation
- C_n^{n0}, $\vec{\omega}_{i/e}^{\,n}$ and $\vec{\omega}_{e/n}^{\,n}$ can be calculated from the vehicle position in earth frame given by a Global Navigation Satellite System (GNSS).

Fig. 2 gives an overview of the algorithm structure. All the steps shown in this figure are further detailed in the following sections.

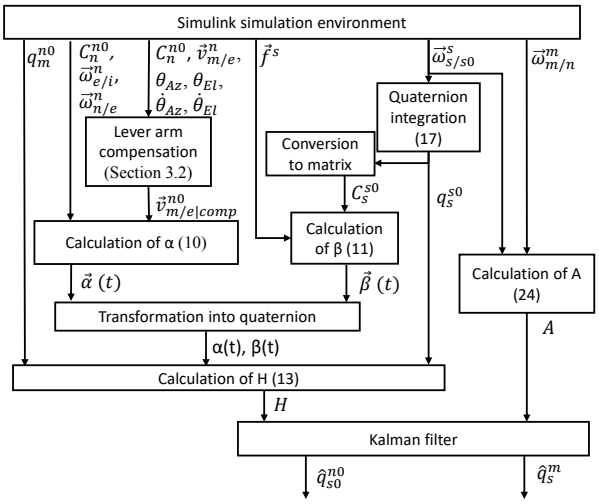

Fig. 2. Block diagram of the transfer alignment algorithm

B. Measurement equation

The method of this work is based on the pseudo-measurement equation explained in [12]. This Section III.B briefly recaps the elements from this former reference that are needed in order to understand the rest of the paper.

The measurement model is a pseudo-measurement equation as all the terms of the measurement vector Y are zeros. In order to get to this, first we define two vectors $\vec{\alpha}$ and $\vec{\beta}$

such as:

$$\vec{\alpha}(t) = \vec{v}^{n0}_{n/e|comp}(t) - \vec{v}^{n0}_{n/e|comp}(0) + \int_0^t C^{n0}_n((2\vec{\omega}^n_{e/i} + \vec{\omega}^n_{n/e}) \times \vec{v}^n_{n/e} - \vec{g}^n)dt \quad (10)$$

$$\vec{\beta}(t) = \int_0^t C^{s0}_s \vec{f}^s dt \quad (11)$$

where $\vec{v}^{n0}_{n/e|comp}$ is the master INS velocity compensated for lever arm effect. Its calculation is detailed in Section III-C. The details of the real-time calculation of (11) are given in Section III-D.

$\alpha(t)$ and $\beta(t)$ are the quaternions associated with vectors $\vec{\alpha}(t)$ and $\vec{\beta}(t)$. We can then write the pseudo-measurement equation:

$$(0_{8\times1}) = \begin{pmatrix} \gamma(\alpha(t)) - \chi(\beta(t)) & 0_{4\times4} \\ \chi(q^{s0}_s) & -\gamma(q^{n0}_m) \end{pmatrix} X. \quad (12)$$

As a conclusion,

$$H = \begin{pmatrix} \gamma(\alpha(t)) - \chi(\beta(t)) & 0_{4\times4} \\ \chi(q^{s0}_s) & -\gamma(q^{n0}_m) \end{pmatrix}. \quad (13)$$

The details of the calculation of q^{s0}_s are given in Section III-D.

C. Lever arm compensation

In (10), $\vec{v}^{n0}_{n/e|comp}$ refers to the velocity of the master INS in reference frame n_0 compensated for level arm effect. $\vec{v}^{n0}_{n/e|comp}$ is an estimation of $\vec{v}^{n0}_{s/e}$, the velocity of the slave IMU in reference frame n_0.

By decomposing $\vec{v}^{n0}_{s/e}$, we get the following:

$$\vec{v}^{n0}_{s/e} = C^{n0}_n(\vec{v}^n_{s/m} + \vec{v}^n_{m/e}) \quad (14)$$

where $\vec{v}^n_{m/e}$ is the master velocity in n frame and is given by the master INS. C^{n0}_n can be calculated knowing the position of the vehicle and the curvature of the Earth. However, $\vec{v}^n_{s/m}$ is unknown and must be calculated. This calculation uses the measurements from the encoders located on the azimuth and elevation axes and the dimensions of the different parts of the APS. The APS configuration is illustrated in Fig. 1.

Let us define the following matrices:

- $R_z(\theta)$ is the matrix expressing the rotation of angle θ about the z axis.
- $R_y(\theta)$ is the matrix expressing the rotation of angle θ about the y axis.

In our application, the dimensions of the vectors $\vec{MA}$, $\vec{AE}$ and $\vec{ES}$ are in the order of one meter.

$\vec{v}^n_{s/m}$ can then be computed through kinematic considerations. Because the azimuth and elevation rotation operate only on one axis, we have $\vec{\omega}^m_{b/m} = \begin{bmatrix} 0 & 0 & \dot{\theta}_{Az} \end{bmatrix}^T$ and $\vec{\omega}^b_{s/b} = \begin{bmatrix} 0 & \dot{\theta}_{El} & 0 \end{bmatrix}^T$, yielding:

$$\begin{aligned}\vec{v}^n_{s/m} = \\ C^n_m(S(\vec{\omega}^n_{m/n})(\vec{MA} + R_z(\theta_{Az})(\vec{AE} + R_y(\theta_{El})\vec{ES}))) \\ + C^n_m R_z(\theta_{Az})(S(\vec{\omega}^m_{b/m})(\vec{AE} + R_y(\theta_{El})\vec{ES})) \\ + C^n_m R_z(\theta_{Az})R_y(\theta_{El})S(\vec{\omega}^b_{s/b})\vec{ES}.\end{aligned} \quad (15)$$

Using (15), the lever arm effect can be compensated knowing the system's dimensions, the vehicle position, and the angular positions and angular rates on the azimuth and elevation axes.

D. Integration

In modern transfer alignment, the computed slave velocity and attitude are accessible measurements, although they contain sensor errors [15], [16], [17]. This is not the case in our application case: the slave IMU only provides rotation rates and acceleration. In order to compute q^{s0}_s in (13) and $\int_0^t C^{s0}_s \vec{f}^s dt$ in (11), these measurements have to be integrated in real time.

Using (1), we write:

$$\dot{q}^{s0}_s = \frac{1}{2} q^{s0}_s \otimes \omega^s_{s/s0}. \quad (16)$$

Since the frame $(s0)$ is immobile relatively to the inertial frame, $\vec{\omega}^s_{s/s0}$ is the output measurement of the slave gyrometers. Equation (16) can therefore be integrated using q^{s0}_s at the previous step to yield q^{s0}_s at the current step.

All that remains is the issue of initialization. Traditional rapid transfer alignment methods such as the one described in [5] calculate the slave attitude, making it necessary to approximate the initial slave attitude with the initial master attitude. Instead, we calculate the slave orientation between its initial attitude and its current attitude. At $t = 0$, the reference frames (s) and $(s0)$ are aligned; therefore, by definition, $q^{s0}_s = \begin{bmatrix} 1 & 0 & 0 & 0 \end{bmatrix}^T$.

C^{s0}_s can be deduced from q^{s0}_s. This allows the integration of the slave accelerometer output as done in (11). It is initialized by $\vec{\beta}(0) = 0$.

Notice that the errors on the measurement of $\vec{\omega}^s_{s/s0}$ and $\vec{f}^s$ due to slave IMU imperfections will accumulate over time, and eventually they may cause these calculations of q^{s0}_s and $\vec{\beta}(t)$ to drift from their real values. On the other hand, transfer alignment algorithms are commonly used for short period of times, which limits the extent of the drift due to error integration; in this work as well, we have verified that within the simulation time, no significant drift has been observed.

E. An innovative propagation equation

[12] made the hypothesis that any variation of X is due solely to process noise. While this is true of $q^{n_0}_{s_0}$ by definition, it is not necessarily the case for q^m_s. In this work's application case, the vehicle motion causes the APS to change the antenna's direction relative to the (m) frame,

so that the antenna's line of sight remains pointed towards the satellite. As a consequence, the (s) frame, aligned with the antenna's line of sight, changes its attitude relatively to (m) frame. The vehicle flexure also impacts the attitude of (s) relative to (m).

We will now develop a propagation model so that the observer can anticipate variations of q_s^m. According to (1), the derivative of q_s^m is as follows:

$$\dot{q}_s^m = \frac{1}{2} q_s^m \otimes \omega_{s/m}^s. \tag{17}$$

The rotation rate $\vec{\omega}_{s/m}^s$ is unknown, so we decompose it:

$$\omega_{s/m}^s = \omega_{s/n}^s - \omega_{m/n}^s \tag{18}$$

where $\vec{\omega}_{s/n}^s$ is the rotation rate provided by the slave IMU. However, $\vec{\omega}_{m/n}^s$ is unknown. Using (2) in (18) yields:

$$\omega_{s/m}^s = \omega_{s/n}^s - q_m^s \otimes \omega_{m/n}^m \otimes q_s^m \tag{19}$$

where $\vec{\omega}_{m/n}^m$ is the rotation rate provided by the master INS. Rewriting (17) using (19) yields:

$$\dot{q}_s^m = \frac{1}{2} q_s^m \otimes (\omega_{s/n}^s - q_m^s \otimes \omega_{m/n}^m \otimes q_s^m). \tag{20}$$

We can then develop this equation. By using (4), the expression becomes:

$$\dot{q}_s^m = \frac{1}{2} (q_s^m \otimes \omega_{s/n}^s - \omega_{m/n}^m \otimes q_s^m). \tag{21}$$

Using (5) and (6), we can put this equation in matrix form:

$$\dot{q}_s^m = \frac{1}{2} (\chi(\omega_{s/n}^s) q_s^m - \gamma(\omega_{m/n}^m) q_s^m). \tag{22}$$

By factorizing this, we can write the propagation model of this rapid transfer alignment algorithm applied to large variable angles:

$$\dot{X} = \begin{pmatrix} 0_{4\times4} & 0_{4\times4} \\ 0_{4\times4} & \frac{1}{2}\chi(\omega_{s/n}^s) - \frac{1}{2}\gamma(\omega_{m/n}^m) \end{pmatrix} X. \tag{23}$$

As a conclusion,

$$A = \begin{pmatrix} 0_{4\times4} & 0_{4\times4} \\ 0_{4\times4} & \frac{1}{2}\chi(\omega_{s/n}^s) - \frac{1}{2}\gamma(\omega_{m/n}^m) \end{pmatrix}. \tag{24}$$

Equation (24) is an innovative propagation model expressing the misalignment quaternion's variations in time, thus extending the model developed in [12] that only applied to constant misalignment angles. If the angle is constant, $(\frac{1}{2}\chi(\omega_{s/n}^s) - \frac{1}{2}\gamma(\omega_{m/n}^m))q_s^m = 0$, yielding the trivial propagation model available in the literature.

IV. Simulation

A. Simulation conditions

A simulation in a MATLAB Simulink environment is used to evaluate the performance of the proposed method. The simulation model includes a ground vehicle, an APS and an antenna, and has it been developed by the company Thales.

The vehicle motion model is based on the work in [18]. Two motion profiles have been simulated: relaxed and extreme off-road conditions. An INS model in (m) frame, a two-axes APS and an IMU in (s) frame then use this motion information to calculate their respective outputs: master velocity, rotation rates and attitude, slave acceleration and rotation rate, and APS axis rotation angles. During the simulated scenario, the APS rotates the antenna until it points towards the satellite, then it keeps it inertially stabilized, causing a misalignement between (m) frame and (s) frame: it is this time-varying misalignement that the present work aims to estimate.

The slave IMU's specifications and noises are given in Table I. The slave IMU runs at 2000 Hz. The master INS is considered ideal and runs at 100 Hz.

TABLE I
Approximate sensor and noise specifications of the slave IMU

Error	Order of magnitude
Accelerometer range	10^2 m/s^2
Accelerometer sensitivity	10^{-8} (m/s^2)/LSB
Accelerometer bias	10^{-2} m/s^2
Accelerometer axes misalignment	10^{-3} rad
Velocity random walk	10^{-4} (m/s^2)/$\sqrt{\text{Hz}}$
Accelerometer bias instability	10^{-3} m/s^2
Gyroscope range	10 rad/s
Gyroscope sensitivity	10^{-8} (rad/s)/LSB
Gyroscope bias	10^{-5} rad/s
Gyroscope axes misalignment	10^{-3} rad
G-sensitivity	10^{-5} (rad/s)/(m/s^2)
Angular random walk	10^{-4} (rad/s)/$\sqrt{\text{Hz}}$
Gyroscope bias instability	10^{-4} rad/s

The Kalman filter noise covariance matrices were determined through empirical testing. The structure of the algorithm, which includes the calculation of the model matrices and Kalman filter, is given in Fig. 2.

The integrations described in (16) and (11) are executed with a three-steps Adams-Bashforth method, more accurate than a forward Euler integration.

B. Simulation results

The initial convergence happens within 2.5 s in relaxed conditions and 15 s in extreme conditions (Fig. 3). This is accomplished without any specific manoeuver from the vehicle.

Two variables are of interest to examine the performance of the proposed solution. One is the estimation error (Fig. 3): the angle between the estimated antenna direction and the actual antenna direction, which we have compared with the one obtained by using the preexisting method developed in [12]. The simulation results show that the estimation error stays beneath $0.22°$ in relaxed off-road conditions, and beneath $1°$ in extreme off-road conditions. In both cases, for the same tuning, the proposed method performs better than the preexisting method. It is important to point out that these results are highly dependent on the choice of the weights of the Kalman filter; in particular for the extreme off-road

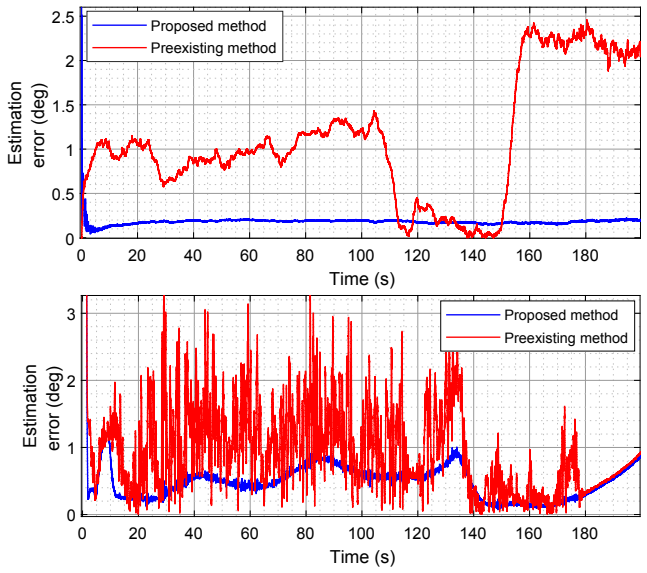

Fig. 3. Amplitude of the angle between estimated antenna direction and actual antenna direction, top: driving in relaxed off-road conditions, bottom: driving in extreme off-road conditions

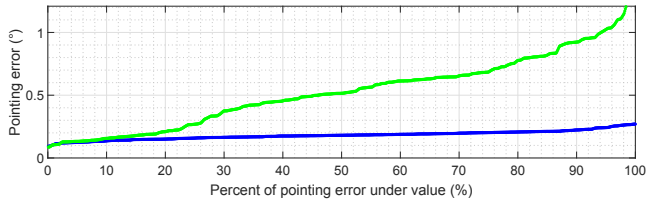

Fig. 4. Cumulative distribution of the pointing error using the proposed solution, in percent of the signal between $t = 0.5$ s and $t = 200$ s (blue: relaxed scenario, green: extreme scenario)

conditions, this tuning has been quite challenging for the pre-existing method (even for achieving these underperforming results), whereas the range of effective Kalman weights for the proposed methods is quite large.

The second variable of interest is the pointing error: in a SOTM simulation similar to the one described in [19], the algorithm results are used to control an APS and to point an antenna towards a satellite. The pointing error is the angle between the target satellite direction and the actual pointed direction, and its cumulative distribution over 200 s is given in Fig. 4. The results show that 95% of the time, the pointing error remains under $0.25°$ in relaxed off-road conditions and $1.02°$ in extreme off-road conditions. From the MIL-STD-188-164 standard [20] and the formula given in [21], we can conclude that this algorithm can be used to point antennas up to 82 cm in diameter when used in relaxed off-road conditions.

V. Conclusion

This paper addresses the problem of estimating a large time-varying misalignment between two inertial platforms. The developed algorithm is an evolution of preexisting algorithms using a linear model and quaternion representation, supplemented with a new propagation model for large time-varying misalignment variations. The simulation results show that the accuracy reached is sufficient for applications such as open-loop Satcom On-The-Move pointing and inertial stabilization.

Future research will look into experimental validation and adaptation of the algorithm to the specific Satcom application.

References

[1] Y. Yüksel, "Design and analysis of transfer aligment algorithms," Master's thesis, Middle East Technical University, 2005.

[2] Y. Lu and X. Cheng, "Random misalignment and lever arm vector online estimation in shipborne aircraft transfer alignment," *Measurement*, vol. 47, pp. 756–764, 2014.

[3] X. Gong and L. Chen, "A conditional cubature Kalman filter and its application to transfer alignment of distributed position and orientation system," *Aerospace Science and Technology*, vol. 95, p. 105405, 2019.

[4] S. Chaudhuri and P. Nandi, "Transfer alignment for space vehicles launched from a moving base," *Defence Science Journal*, vol. 55, no. 3, p. 245, 2005.

[5] J. Kain and J. Cloutier, "Rapid transfer alignment for tactical weapon applications," in *Guidance, Navigation and Control Conference*, 1989, p. 3581.

[6] Z. Xiong, F. Sun, and Q. Nie, "Observability analysis of INS rapid transfer alignment," in *2006 6th World Congress on Intelligent Control and Automation*, vol. 1, June 2006, pp. 1664–1668.

[7] G. Xu, Y. Huang, Z. Gao, and Y. Zhang, "A computationally efficient variational adaptive Kalman filter for transfer alignment," *IEEE Sensors Journal*, vol. 20, no. 22, pp. 13 682–13 693, Nov 2020.

[8] X. Chen, Z. Ma, and P. Yang, "Integrated modeling of motion decoupling and flexure deformation of carrier in transfer alignment," *Mechanical Systems and Signal Processing*, vol. 159, p. 107690, 2021.

[9] J. Cheng, T. Wang, D. Guan, and M. Li, "Polar transfer alignment of shipborne SINS with a large misalignment angle," *Measurement Science and Technology*, vol. 27, no. 3, p. 035101, jan 2016.

[10] X. Cui, C. Mei, Y. Qin, G. Yan, and Z. Liu, "A unified model for transfer alignment at random misalignment angles based on second-order EKF," *Measurement Science and Technology*, vol. 28, no. 4, p. 045106, feb 2017.

[11] S. Zhou, H. Xu, H. Dai, and G. Wu, "Novel rapid transfer alignment algorithm for strapdown inertial navigation system," in *2011 International Conference on Electrical and Control Engineering*, Sep. 2011, pp. 6012–6016.

[12] Y. Chen and Y. Zhao, "New rapid transfer alignment method for SINS of airborne weapon systems," *Journal of Systems Engineering and Electronics*, vol. 25, no. 2, pp. 281–287, April 2014.

[13] J. DeBruin, "Control systems for mobile Satcom antennas," *IEEE Control Systems Magazine*, vol. 28, no. 1, pp. 86–101, Feb 2008.

[14] H. Parwana and M. Kothari, "Quaternions and attitude representation," *arXiv:1708.08680*, 2017.

[15] J. Cheng, J. Cai, Z. Wang, and J. Liu, "A novel polar rapid transfer alignment for shipborne SINS under arbitrary misalignments," *IEEE Access*, vol. 8, pp. 197 567–197 580, 2020.

[16] J. Cai, J. Cheng, J. Liu, Z. Wang, and Y. Xu, "A polar rapid transfer alignment assisted by the improved polarized-light navigation," *IEEE Sensors Journal*, vol. 22, no. 3, pp. 2508–2517, Feb 2022.

[17] W. Lyu, X. Cheng, and J. Wang, "Adaptive UT-H_∞ filter for SINS' transfer alignment under uncertain disturbances," *IEEE Access*, vol. 8, pp. 69 774–69 787, 2020.

[18] M. Alazab Elkhouly, "Standardized testing conditions for satellite communications on-the-move (SOTM) terminals," Ph.D. dissertation, Technische Universität Ilmenau, 2018.

[19] E. Broussard, M. T. Pham, M. Ladevez, X. Brun, and B. Vion, "Hybrid satellite position estimator using self-induced dither for SATCOM on the Move," in *20th IFAC World Congress*, Toulouse, France, Jul 2017, pp. 7208–7212.

[20] NPFC, *MIL-STD-188-164: Interoperability of SHF satellite communications Earth terminals*, Naval Publications and Form Center Std., November 2018.

[21] J. Laine, "2D model-based step-track procedure," *IEEE Transactions on Aerospace and Electronic Systems*, vol. 36, no. 4, pp. 1386–1391, Oct 2000.